

Resonance states of unnatural parity in positronic atoms

Isao Shimamura*

Atomic Physics Laboratory, RIKEN, Wako, Saitama 351-0198, Japan

and Advanced Science Research Center, Japan Atomic Energy Agency, Tokai-mura, Naka-gun, Ibaraki 319-1195, Japan

Hiroaki Wakimoto and Akinori Igarashi

Department of Applied Physics, Miyazaki University, Miyazaki 889-2192, Japan

(Received 3 August 2009; published 17 September 2009)

Resonance states of unnatural parity P^e and D^o in the positronic atoms e^+H and e^+He^+ are calculated and discussed in detail in terms of the coupled-channel scheme in the hyperspherical coordinate system. New resonances emerge in the analysis of the eigenphase sum. The time-delay matrix eigenvalues prove to be useful in unraveling overlapping resonances. Many resonances are identified as belonging to some infinite series of Feshbach resonances supported by an adiabatic hyperspherical potential. Some Feshbach resonances independent of any infinite series are also identified to be supported by an adiabatic potential. The positions and widths of higher-lying members of the infinite series are known to be expressible as geometric progressions. Their common ratios are obtained theoretically, including those for the series failing to appear in the present calculation. Several resonances unassociated with a minimum in any adiabatic potential are found in the region of avoided crossing. The diabatic picture is invoked for understanding the resonance mechanism, the resonance energy, and the trend in the widths for all those exceptional cases. The lowest-order 2γ and 3γ pair annihilation in these unnatural-parity states is shown to be forbidden.

DOI: [10.1103/PhysRevA.80.032708](https://doi.org/10.1103/PhysRevA.80.032708)

PACS number(s): 34.80.Uv, 34.80.Lx, 31.15.xj

I. INTRODUCTION

The excited state $H^-(2p^2\ ^3P^e)$ of the hydrogen negative ion has an energy slightly below the threshold of electron detachment into the continuum $H(2s, 2p)+e^-$ but well above the threshold for the continuum $H(1s)+e^-(l)$ [1]. Nevertheless, it is a true bound state rather than a resonance state; autodetachment into the only continuum $H(1s)+e^-(p)$ with no change in the orbital angular momentum $L (=1)$ is forbidden since the parity would necessarily change into odd by this electron detachment (parity forbidden). This state $H^-(2p^2\ ^3P^e)$ is an example of unnatural parity, $\pi=(-1)^{L+1}$.

Systems containing positronium Ps, consisting of an electron e^- and a positron e^+ , afford other examples. Excited states $PsH(^{2,4}S^o)$ of the positronium hydride having an energy slightly below the threshold for dissociation into $H(2p)+Ps(2p)$ but above the thresholds for a few continuum channels have been found in elaborate calculations [2,3]. These states are true bound states since both autodissociation and autoionization with no change in L are parity forbidden. Also, the electron-positron pair annihilation in them by the normal 2γ or 3γ emission in the lowest order is forbidden [2,3]. The lowest-order 2γ annihilation occurs for a singlet s e^-e^+ pair with a rate of about the order of $10^9\ s^{-1}$ in normal atoms and small molecules and the lowest-order 3γ annihilation occurs for a triplet s pair with a rate three orders of magnitude slower. These rates are proportional to the expectation value of the delta function $\delta(\mathbf{r})$ of the e^-e^+ distance vector \mathbf{r} . This expectation value vanishes if the internal motion of the e^-e^+ pair has a nonzero orbital angular momentum, as is the case with $PsH(^{2,4}S^o)$.

Such unusual states are of recent particular interest, and some other positron-involving slightly bound states of unnatural parity in PsLi, PsNa, and PsK have been studied theoretically in the frozen-core approximation, which renders the difficult many-body problem into an approximate four-body problem [2,3]. Among these states, the PsLi has been identified to be an example of a peculiar Boromean state [4,5], with the constituent four “particles” (Li^+ , e^- , e^- , and e^+) being able to form no stable three-body bound state that can be a parent for the four-body $^{2,4}S^o$ state.

Unnatural-parity resonance states in positronic systems e^+H [6] and e^+He^+ [7] have also been calculated recently using the complex-coordinate rotation method. This theoretical technique changes the complicated continuum-state problem into a bound-state problem in the complex-coordinate space. It thus avoids the calculation of the continuum wave function with the correct asymptotic channels that yields scattering parameters, such as the scattering matrix S . Instead, each complex-energy eigenvalue $E_r - i(\Gamma/2)$ is directly calculated one by one, where E_r is the energy position of a resonance and Γ is its resonance width. Computed values of (E_r, Γ) are reported in Refs. [6,7].

The present work is motivated to unravel the physics of these unnatural-parity resonances in e^+H and e^+He^+ by exploiting the hyperspherical close-coupling (HSCC) method, a continuum multichannel technique briefly introduced in Sec. II. The resonance parameters are extracted from the S matrix, as is explained in Sec. IV. The HSCC method has an advantage of specifying the mechanisms for many of the resonances, identifying them as supported by particular adiabatic potential energy curves $U_i(\rho)$ in the hyper-radius ρ (to be explained in Sec. II) and as modified by the nonadiabatic coupling between these adiabatic hyperspherical channels (Secs. VI A and VI B). In fact, the system e^+He^+ has two different kinds of asymptotic channels, one with the repul-

*shimamura@ribf.riken.jp

sive Coulomb potential between e^+ and $\text{He}^+(n, l)$ and the other with a nearly constant potential between $\text{Ps}(n', l')$ and He^{2+} (Sec. VI). These two kinds of channels produce many avoided crossings, which expectedly lead to rich and complicated multichannel physics. Indeed, the *adiabatic* picture proves to be crucial in the region of avoided crossings between the adiabatic curves, as is discussed in Sec. VI C.

The multichannel technique can also be used to understand the infinite series of Feshbach resonances supported by the asymptotic dipole potential in the nonrelativistic framework (see Sec. V). This theory is useful in analyzing many resonances in Sec. VI B. Another conspicuous point to notice in Sec. III is that the lowest-order 2γ and 3γ annihilation is forbidden in the unnatural-parity states of the system $e^+\text{H}$ or $e^+\text{He}^+$.

Atomic units are used throughout this paper.

II. HYPERSPHERICAL COUPLED-CHANNEL METHOD

Both systems $e^+\text{H}$ and $e^+\text{He}^+$ consist of a positron, an electron, and a nucleus, either a proton p or an alpha particle He^{2+} . The Schrödinger equation with the exact three masses is expressible in terms of the Jacobi coordinates, e.g., \mathbf{r}_- for e^- relative to the nucleus and \mathbf{r}_+ for e^+ relative to the center of mass of the hydrogen atom or the helium ion He^+ . For an accurate numerical solution of the Schrödinger equation for a strongly correlated three-body system and for transparent elucidation of its dynamics, the hyperspherical coordinate system (ρ, Ω) is now widely accepted as much more suitable than the pair $(\mathbf{r}_-, \mathbf{r}_+)$ of the conventional Jacobi coordinates [8,9]. The hyper-radius ρ is defined by

$$\rho^2 = \mu_- r_-^2 + \mu_+ r_+^2, \quad (1)$$

where μ_- and μ_+ are the reduced masses corresponding to the motion in r_- and in r_+ and are both close to the electron mass of 1.0. The hyper-radius is a measure of the size of the whole three-body system. This variable represents the two light particles collectively and nearly on a par. It allows a part of the correlation effects to be described efficiently. The hyperangle Ω denotes the five angular coordinates $(\xi, \hat{\mathbf{r}}_+, \hat{\mathbf{r}}_-)$ collectively, where $\tan \xi = \mu_-^{1/2} r_- / \mu_+^{1/2} r_+$. A remarkable theoretical advantage, not enjoyed by using the conventional coordinate system, is that only one variable out of the six-dimensional coordinate space runs over to infinity and the five other variables run over a finite region.

The fragmentation channel $e^+\text{H}$ (He^+) is associated with the coordinate region $(\rho \gg 1, \xi \ll 1)$. The fragmentation channel $\text{Ps}+\text{H}^+$ (He^{2+}) would be described more appropriately by the hyper-radius ρ' defined in terms of \mathbf{r} , the internal coordinate of Ps, and \mathbf{R} , the position vector of the nucleus relative to the center of mass of Ps; $\rho'^2 = \mu_r r^2 + \mu_R R^2$. Here, μ_r (≈ 0.5) is the reduced mass of Ps and μ_R (≈ 2.0) is that associated with the motion in \mathbf{R} . In fact, this new hyper-radius ρ' turns out to be identical to ρ defined by Eq. (1). Thus, the hyper-radius ρ proves convenient as a reaction coordinate that connects smoothly and naturally the two different classes of fragmentation channels. The five-dimensional hyperangle Ω that is equivalent to the already defined one is expressible as $(\eta, \hat{\mathbf{R}}, \hat{\mathbf{r}})$ with $\tan \eta = \mu_r^{1/2} r / \mu_R^{1/2} R$. The Ps-

nucleus fragmentation is associated with the coordinate region $(\rho \gg 1, \eta \ll 1)$.

The adiabatic hyperspherical states $\varphi_i(\Omega; \rho)$ in the five-dimensional space Ω are calculated as the eigenfunctions of the adiabatic Hamiltonian $H_{\text{ad}}(\Omega; \rho)$, which follows by treating ρ as the adiabatic parameter rather than a variable. Their energies, augmented by the (mock) centrifugal potential coming from the five-dimensional angular part of the kinetic energy operator, are referred to as the adiabatic hyperspherical potentials $U_i(\rho)$. They serve well in understanding the physics of bound and resonance states supported by these potentials, both visually and numerically, in analogy with the adiabatic potentials of diatomic molecules.

For accurate numerical calculations, the wave function $\Psi(\rho, \Omega)$ for the total three-body system is expressed as a linear combination of the adiabatic states in the form

$$\Psi(\rho, \Omega) = \sum_i \rho^{-5/2} F_i(\rho) \varphi_i(\Omega; \rho). \quad (2)$$

Here, the factor $\rho^{-5/2}$ has been introduced for simplification of the explicit form of the coupled equations,

$$\left(-\frac{1}{2} \frac{d^2}{d\rho^2} + U_i(\rho) - E \right) F_i(\rho) + \sum_j V_{ij}(\rho) F_j(\rho) = 0, \quad (3)$$

for the unknown channel functions $F_i(\rho)$. These equations, called the hyperspherical coupled-channel or close-coupling (HSCC) equations, follow from the three-body Schrödinger equation in (ρ, Ω) for a total energy E , where Eq. (2) is substituted. No approximation has been made so far, provided the expansion [Eq. (2)] includes all the basis functions $\{\varphi_j\}$ in the complete set, i.e., provided all the channels are included in Eq. (3). The nonadiabatic coupling $V_{ij}(\rho)$ stems from the kinetic energy operator in ρ , omitted in the adiabatic Hamiltonian $H_{\text{ad}}(\Omega; \rho)$. It includes both a mere multiplicative potential and a first-order differential operator in ρ . For further detail of the HSCC formulation, see Refs. [10,11].

In the present calculations, we retain all open channels and some closed channels in the HSCC equations [Eq. (3)], often confirming the convergence of the resonance parameters (obtained as explained in Sec. IV) with the increase in the number of coupled channels. The much more rapid convergence rate than the conventional close-coupling equations in terms of the independent-particle coordinates is one of the well-established advantages of the HSCC equations. The equations are solved up to a large value of ρ , and then, the solutions are matched with the asymptotic wave function in the coordinates $(\mathbf{r}_-, \mathbf{r}_+)$ or (\mathbf{r}, \mathbf{R}) , satisfying the ordinary scattering boundary conditions. This leads to the scattering matrix $S(E)$. Detailed numerical procedures are elaborated in previous work, which reports successful applications of the HSCC method (see, e.g., Refs. [12–16]).

III. ANNIHILATION IN POSITRONIC ATOMS OF UNNATURAL PARITY

A three-body system with an orbital angular momentum \mathbf{L} and an unnatural parity $\pi = (-1)^{L+1}$ is impossible to form by

coupling a vanishing angular momentum $\mathbf{l}=0$ with another angular momentum \mathbf{l}' since $\mathbf{L}=\mathbf{l}'$, then, and the parity is $(-1)^{l'}=(-1)^L$. If the wave function is written in terms of a set of Jacobi coordinates (\mathbf{x}, \mathbf{X}) , for example, and if it is independent of the angular coordinates $\hat{\mathbf{x}}$ (vanishing angular momentum associated with \mathbf{x}), then this state is of natural parity. Thus, any three-body state of unnatural parity can never break up into a particle and a two-body system in an s state.

Similarly, no unnatural-parity state of the system e^+H or e^+He^+ has an s -state component in the partial-wave expansion of the wave function in the e^-e^+ angular coordinate $\hat{\mathbf{r}}$. Therefore, the lowest-order 2γ and 3γ annihilation is forbidden in the unnatural-parity states. In other words, in-flight or collisional pair annihilation practically never occurs in positron encounters with the hydrogen atoms or the helium ions He^+ (or in positronium encounters with protons or alpha particles), whether via resonance states or not, if the total system is of unnatural parity. Only much slower higher-order annihilation can occur in the positronium, if any, after the collision.

IV. RESONANCE FITTING

The scattering matrix $S(E)$ contains the information on resonances, as well as, unlike the complex-coordinate rotation calculations, nonresonant background and its interference with the resonances. The eigenphases are determined by diagonalizing the S matrix, and sharp structures in their sum $\delta(E)$ are located. To their energy dependence the Breit-Wigner one-level formula [17,18],

$$\delta(E) = \arctan \frac{\Gamma/2}{E_r - E} + \delta_b(E), \quad (4)$$

is fitted with the background phase $\delta_b(E)$ usually assumed to be linear in E (or quadratic in E in some cases of broad resonances). This simple fitting procedure normally works well for deriving the resonance parameters (E_r, Γ) .

Very broad resonances and overlapping resonances require careful analysis. For this purpose, the time-delay matrix $Q(E)$, introduced by Smith [19] and related to the S matrix by $Q(E)=iS(\partial S^\dagger/\partial E)$, proved to be useful [20–22]. Its trace, $\text{Tr } Q(E)$, or the diagonal sum satisfies the relation [21]

$$\begin{aligned} \text{Tr } Q(E) &= \sum_i Q_{ii}(E) = \sum_i q_i(E) = 2 \frac{\partial \delta}{\partial E} \\ &= \sum_\nu \frac{\Gamma_\nu}{(E - E_{r,\nu})^2 + (\Gamma_\nu/2)^2} + 2 \frac{\partial \delta_b(E)}{\partial E}. \end{aligned} \quad (5)$$

Here, the summation of the Lorentzians over more than one resonance has been introduced to cover overlapping resonances as well. According to Eq. (5), $\text{Tr } Q(E)$ provides information equivalent to $\delta(E)$. The inspection of the eigenvalues $q_i(E)$ of the Q matrix, however, singles out each resonance clearly [20–22].

Figure 1(a) illustrates the Q -matrix eigenvalues and their sum for the $e^+He^+(P^e)$ resonance found near the threshold -0.079989 of $e^+ + He^+(n=5)$. The center of the Lorentzian lies below this threshold by only $\sim 3 \times 10^{-3}$, but its width

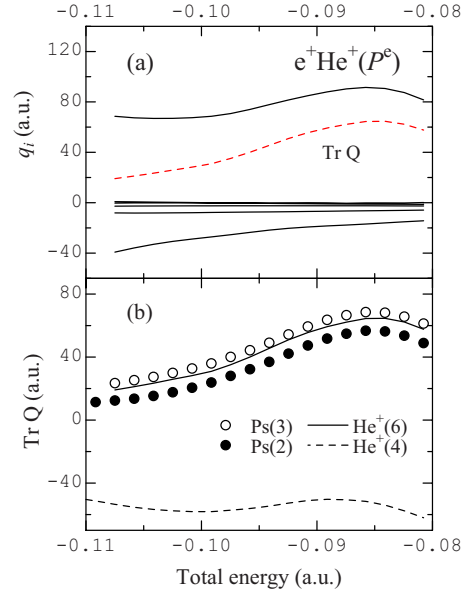


FIG. 1. (Color online) (a) Eigenvalues $q_i(E)$ of the time-delay matrix $Q(E)$ for $e^+He^+(P^e)$ and their sum, $\text{Tr } Q(E)$. (b) Convergence of $\text{Tr } Q(E)$ as the number of HSCC equations increases. $He^+(n)$ and $Ps(n)$ stand for coupling all channels up to those producing asymptotically $He^+(n)$ and $Ps(n)$.

0.034 covers a strikingly broad energy range across this threshold. This resonance is discussed in the last part of Sec. VI C. Figure 1(b) shows the convergence behavior of $\text{Tr } Q(E)$. Coupling all the channels up to those breaking up asymptotically into $e^+ + He^+(n=4)$ is seen to be far from convergence, but further inclusion of all the channels breaking up into $e^+ + He^+(n=5)$ and into $He^{2+} + Ps(n=2)$ is already good enough for extracting accurate resonance parameters.

A remarkable case of overlapping resonance is found in Fig. 2. One of the Q -matrix eigenvalues is by far the largest and almost coincides with $\text{Tr } Q(E)$ [see Fig. 2(a)]. Fitting the Breit-Wigner formula [Eq. (5)] to it reveals only one resonance. By enlarging the scale and paying attention to the much smaller second largest eigenvalue, as in Fig. 2(b), one finds another weak and broad peak overlapping the conspicuous one. It might look like a mere background. However, it is clearly a Lorentzian. Also, the extracted resonance energy and width agree quite well with a complex pole of the S matrix calculated in a completely different manner by the complex-coordinate rotation technique [7]. This will be seen in Table III to be presented later in Sec. VI. Furthermore, this broad resonance will turn out in Sec. VI C to be a member of an infinite series supported by some potential. Figure 2(c) shows a close agreement between the results with different numbers of coupled equations, showing the near convergence attained.

V. INFINITE SERIES OF FESHBACH RESONANCES

In terms of the conventional Jacobi coordinates, the potential matrix elements in the close-coupling equations for the systems e^+H and e^+He^+ have an asymptotic form $\sim \alpha_{ij}/(2X^2)$ except for those associated with the fragmenta-

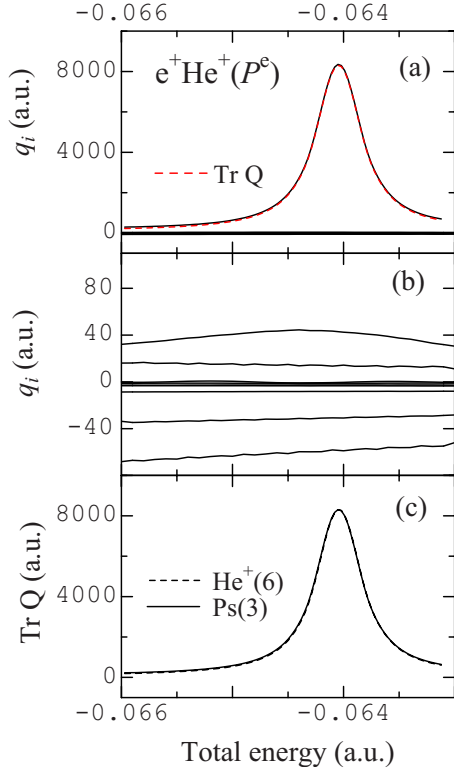


FIG. 2. (Color online) (a) Eigenvalues $q_i(E)$ of the time-delay matrix $Q(E)$ for $e^+\text{He}^+(P^e)$ and their sum, $\text{Tr } Q(E)$, which is almost the same as the largest eigenvalue. (b) Eigenvalues $q_i(E)$ on an enlarged scale to distinguish between the smaller eigenvalues. (c) Convergence of $\text{Tr } Q(E)$ as the number of HSCC equations increases. $\text{He}^+(6)$ and $\text{Ps}(3)$ stand for coupling all channels up to those producing asymptotically $\text{He}^+(n=6)$ and up to $\text{Ps}(n=3)$. Both results are almost indistinguishable.

tion channels $e^+\text{He}^+$ with a repulsive Coulomb tail. Here, X is either $\mu_+^{1/2}r_+$ or $\mu_R^{1/2}R$. The diagonal elements $\alpha_{ii}/(2X^2)$ represent the centrifugal potential. The off-diagonal dipole potentials $\alpha_{ij}/(2X^2)$ stem from the dipole coupling between channels producing a two-body fragment with angular momentum differing by one unit, for example, p - d coupling. No fragmentation of an unnatural-parity three-body state produces a two-body fragment in an s state, as noted in Sec. III. Therefore, no two-body systems are produced in the ground state. Also, no asymptotic s - p coupling occurs, and hence, no off-diagonal dipole potential exists for the $n=2$ unnatural-parity channels.

The coefficient α_{ij} may be positive, negative, or vanishing. In the asymptotic limit $X \rightarrow \infty$, the dipole potential submatrix $\{\alpha_{ij}\}/(2X^2)$ within a set of degenerate channels may be diagonalized by a unitary transformation, so that the transformed asymptotic channels are decoupled. Any dipole potential for a decoupled channel having a coefficient α (here called a dipole-moment eigenvalue) less than $-1/4$ is known to support an infinite number of bound-state levels converging to the asymptotic energy of those degenerate channels. These bound states turn into an infinite series of Feshbach resonances via coupling with open channels [23]. The relativistic effects actually terminate the series at some finite number. There may also be shape and Feshbach resonances that are independent of any series.

TABLE I. Parameters for the infinite series of Feshbach resonances of symmetries P^e and D^o in the systems $e^+\text{H}$ and $e^+\text{He}^+$. E_{th} : series limit. α : dipole-moment eigenvalue (less than $-1/4$). C : parameter appearing in Eq. (6) for the resonance positions and widths.

| System | Fragmentation | E_{th} | Symmetry | α | C |
|--------------------|---------------------------------|-----------------|----------|----------|----------|
| $e^+\text{H}$ | $e^+\text{H}(n=5)$ | -0.019989 | P^e | -37.70 | 1.027 |
| | | | P^e | -3.482 | 3.495 |
| | | | D^o | -35.05 | 1.065 |
| | $p+\text{Ps}(n=3)$ | -0.027778 | D^o | -20.14 | 1.409 |
| | | | D^o | -0.458 | 13.78 |
| | | | P^e | -32.02 | 1.115 |
| $e^+\text{H}(n=4)$ | -0.031233 | D^o | -28.25 | 1.187 | |
| | | P^e | -18.46 | 1.472 | |
| $e^+\text{H}(n=3)$ | -0.055525 | D^o | -15.72 | 1.597 | |
| | | D^o | -4.840 | 2.933 | |
| $e^+\text{He}^+$ | $\text{He}^{2+}+\text{Ps}(n=3)$ | -0.027778 | P^e | -68.01 | 0.7633 |
| | | | D^o | -64.12 | 0.7862 |

Table I summarizes the dipole-moment eigenvalues α ($< -1/4$) for infinite series in unnatural-parity $e^+\text{H}$ and $e^+\text{He}^+$. Clearly, there are no infinite series converging to the threshold of $e^+\text{H}(n=2)$ or of p (or $\text{He}^{2+})+\text{Ps}(n=2)$ because of the absence of the s - p coupling. This differentiates unnatural-parity resonances from natural-parity resonances. The table says, for example, that there exist two $e^+\text{H}(P^e)$ and three $e^+\text{H}(D^o)$ series converging to an energy of -0.019989 a.u., i.e., the threshold of the continuum $e^+\text{H}(n=5)$.

The resonance parameters for the higher members (labeled by an integer ν) of an infinite series converging to a threshold energy E_{th} may be expressible as [23]

$$E_{r,\nu} = E_{\text{th}} - \varepsilon_\nu, \quad \varepsilon_\nu = \varepsilon_0 \exp(-C\nu),$$

$$\Gamma_\nu = \Gamma_0 \exp(-C\nu). \quad (6)$$

Here, the constant C is common to both the resonance positions and widths for each series. It is calculable from the dipole-moment eigenvalue and is included in Table I. The constants ε_0 and Γ_0 depend on the whole interaction including the short-range potentials, and their determination requires a full resonance calculation.

VI. ANALYSIS OF THE RESONANCES

The positions and widths of the resonances found in the system $e^+\text{H}$ are summarized in Table II and those found in the system $e^+\text{He}^+$ in Table III. Some of those resonances were also calculated previously by using the complex-coordinate rotation method [6,7], and the results are reproduced in these tables. The threshold energies E_{th} included in these tables are for the exact reduced mass, as is used in the

TABLE II. Energies E_r and widths Γ of P^e and D^o resonances in e^+H . $x[y]=x \times 10^y$. E_{th} represents the threshold energy.

| Threshold, E_{th} | P^e | | D^o | |
|--------------------------|------------------------------------|--|------------------------------------|--|
| | HSCC ^a E_r, Γ | Complex rotation ^b E_r, Γ | HSCC ^a E_r, Γ | Complex rotation ^b E_r, Γ |
| Ps($n=4$), -0.015625 | | | | |
| H($n=5$), -0.019989 | | | $-0.02018, 2.6[-6]$ | |
| | $-0.02026, 8.82[-6]$ | | $-0.02022, 8.6[-6]$ | |
| | $-0.02078, 2.19[-5]$ | | $-0.02068, 2.3[-5]$ | |
| | | | $-0.02084, 1.2[-5]$ | |
| | $-0.02236, 4.60[-5]$ | | $-0.02217, 5.2[-5]$ | |
| Ps($n=3$), -0.027778 | | | | |
| | $-0.02785, 1.21[-5]$ | | $-0.02782, 6.6[-6]$ | |
| | $-0.02799, 3.74[-5]$ | | $-0.02793, 2.2[-5]$ | |
| | $-0.02845, 1.21[-4]$ | | $-0.02830, 7.4[-5]$ | |
| | $-0.02988, 4.07[-4]$ | | $-0.02957, 2.5[-4]$ | |
| H($n=4$), -0.031233 | | | | |
| | $-0.03128, 1.3[-6]$ | | | |
| | $-0.03143, 5.2[-6]$ | $-0.03145, 7.0[-6]$ | $-0.03135, 1.7[-6]$ | $-0.03138, 5.0[-6]$ |
| | | | $-0.03154, 2.0[-5]$ | $-0.03162, 2.2[-5]$ |
| | $-0.03211, 1.9[-5]$ | $-0.03215, 1.9[-5]$ | $-0.03186, 9.9[-6]$ | $-0.03190, 1.0[-5]$ |
| | $-0.03552, 4.6[-5]$ | $-0.03558, 4.6[-5]$ | $-0.03485, 3.0[-5]$ | $-0.03492, 3.0[-5]$ |
| H($n=3$), -0.055525 | | | | |
| | $-0.05554, 5.6[-8]$ | | | |
| | $-0.05580, 1.2[-6]$ | $-0.05583, 1.2[-6]$ | $-0.05555, 3.8[-6]$ | $-0.05557, 1.0[-6]$ |
| Ps($n=2$), -0.062500 | | | | |
| | $-0.06364, 4.3[-6]$ | $-0.06366, 4.1[-6]$ | | |
| H($n=2$), -0.124932 | | | | |

^aPresent calculation.

^bReference [6].

present hyperspherical calculations. On the other hand, the nucleus was fixed in space in the complex-rotation calculation in Refs. [6,7]. The slight difference between our resonance positions and those in Refs. [6,7] arises partly from the mass-polarization effect.

The adiabatic hyperspherical potentials for e^+H with symmetries P^e and D^o are shown as full curves in Figs. 3 and 4 and those for e^+He^+ in Figs. 5 and 6. The potential-curve structure is similar for both symmetries P^e and D^o for the same system, but the D^o curves naturally lie higher than the P^e curves because of the centrifugal potential and have shallower minimum if any. Therefore, most D^o resonances are found to be shifted slightly upward from those for P^e . In some cases the resonance disappears as the angular momentum increases. The corresponding P^e and D^o resonances are listed in the same row in Tables II and III. In addition, new resonances occur for D^o that have no P^e counterparts. They are introduced by the additional D^o potential curves; note the existence of more D^o curves than P^e curves in Figs. 3–6. Those additional curves are the reason for the more D^o series than P^e series in Table I in spite of the higher centrifugal potential for D^o than for P^e .

Complicated dynamics of e^+He^+ is expected from the many more avoided crossings than for e^+H in the energy region of the potentials breaking up into Ps(n)+He²⁺. These potentials are nearly flat asymptotically. On the other hand, the asymptotic potentials e^+He^+ are repulsive and hence diabatically cross the former potentials and adiabatically avoid crossing them. Most avoided crossings look as if they were real crossings. In other words, strong avoided crossing occurs only for exceptional pairs of diabatic states. Especially, for two diabatic channels with different arrangements crossing at large ρ , the electron lies at quite distant positions in the space, one close to the nucleus and the other close to the positron and far from the nucleus, so that the coupling between these channels should be very weak.

The broken curves will be explained and used for resonance mechanism analysis in Sec. VI C. The calculated resonance energies are indicated by horizontal bars in Figs. 3–6 and are discussed in the following.

A. Nondipole independent Feshbach resonances

The continuous spectrum of the system e^+H of unnatural parity starts at the energy level of H($n=2$). The adiabatic

TABLE III. Energies E_r and widths Γ of P^e and D^o resonances in $e^+\text{He}^+$. $x[y]=x \times 10^y$. The resonance energies are arranged relative to the threshold energies E_{th} , but the broad resonances extending across the threshold $\text{He}^+(n=5)$ are listed in the same row as this threshold in spite of their central positions E_r .

| Threshold, E_{th} | P^e | | D^o | |
|-------------------------------|---|--|---|--|
| | HSCC ^a E_r, Γ | Complex rotation ^b E_r, Γ | HSCC ^a E_r, Γ | Complex rotation ^b E_r, Γ |
| $\text{Ps}(n=3), -0.027778$ | -0.02828, 2.9[-5] -0.02890, 6.1[-5] -0.03037, 1.2[-4] | | -0.02822, 1.9[-5] -0.02879, 4.5[-5] -0.03022, 1.5[-4] | |
| $\text{He}^+(n=8), -0.031246$ | -0.03423, 1.2[-4] | -0.03426, 1.23[-4] | -0.03396, 1.5[-4] | -0.03400, 1.48[-4] |
| $\text{He}^+(n=7), -0.040811$ | -0.0438, 4.1[-3] | -0.04379, 3.99[-2] | -0.04346, 4.6[-3] | -0.04343, 4.56[-3] |
| $\text{He}^+(n=6), -0.055548$ | | | | |
| $\text{Ps}(n=2), -0.062500$ | -0.06404, 4.7[-4] -0.0640, 1.4[-2] | -0.06405, 4.75[-4] -0.0643, 1.8[-2] | -0.06296, 6.2[-4] -0.063, 1.7[-2] | -0.06297, 6.3[-4] -0.06390, 1.98[-2] |
| $\text{He}^+(n=5), -0.079989$ | -0.0833, 3.4[-2] | -0.08411, 3.34[-2] | -0.0790, 4.0[-2] | -0.08083, 3.99[-2] |
| $\text{He}^+(n=4), -0.124983$ | | | | |

^aPresent calculation.

^bReference [7].

potentials in Fig. 3 (P^e) and Fig. 4 (D^o) tending asymptotically to this threshold are repulsive. Hence, these potentials support no bound states below this threshold and no resonances immediately above it. All the potentials in Figs. 5 and 6 tending to the $\text{He}^+(n=2, 3, 4)$ thresholds are also repulsive because of the Coulomb potential between e^+ and He^+ . These potentials remain repulsive at short distances ρ . Thus, no bound states are found below the continuum threshold $\text{He}^+(n=2)$ and no resonances are found below the thresholds $\text{He}^+(n=3, 4)$.

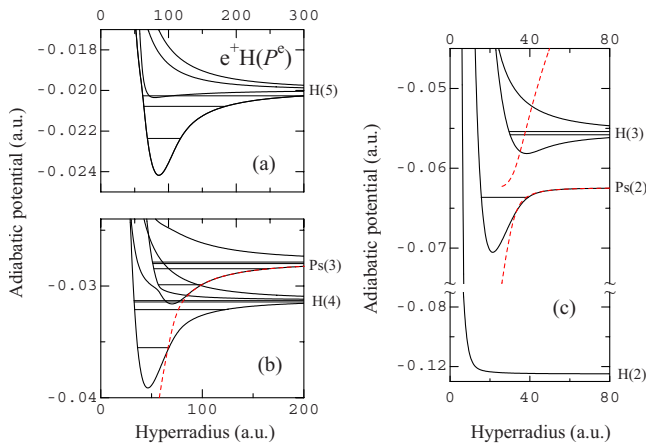


FIG. 3. (Color online) Adiabatic hyperspherical potentials (full curves) of the system $e^+\text{H}(P^e)$ as functions of the hyper-radius ρ . The broken curves are for the $p+\text{Ps}$ configurations only and are explained in Sec. VI C. The vertical positions of the symbols $\text{H}(n)$ and $\text{Ps}(n)$ on the right roughly indicate these asymptotic threshold energies. The calculated resonance levels are shown by horizontal bars.

The $e^+\text{H}(P^e)$ potential approaching the threshold $\text{Ps}(n=2)$ has a minimum and supports a bound state, as indicated by a horizontal bar, which turns into a Feshbach resonance below this threshold. For D^o , this minimum is too shallow to support a resonance. For $e^+\text{He}^+$, this potential shows a strong avoided crossing with a $e^++\text{He}^+$ potential, which complicates the dynamics. A similar situation occurs also for the $\text{Ps}(n=3)$ potentials. These cases are discussed in detail in Sec. VI C.

B. Infinite series of dipole resonances

The asymptotic potentials in Figs. 3–6 are almost the same as the decoupled dipole potentials in the diagonalized

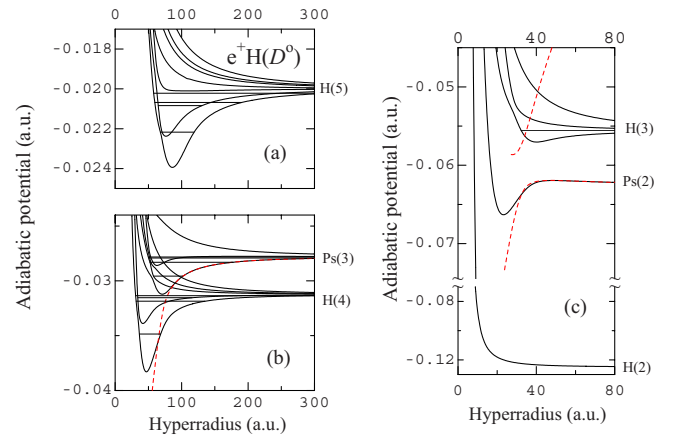


FIG. 4. (Color online) Adiabatic hyperspherical potentials (full curves) of the system $e^+\text{H}(D^o)$ as functions of the hyper-radius ρ . For the broken curves and horizontal bars, see caption of Fig. 3.

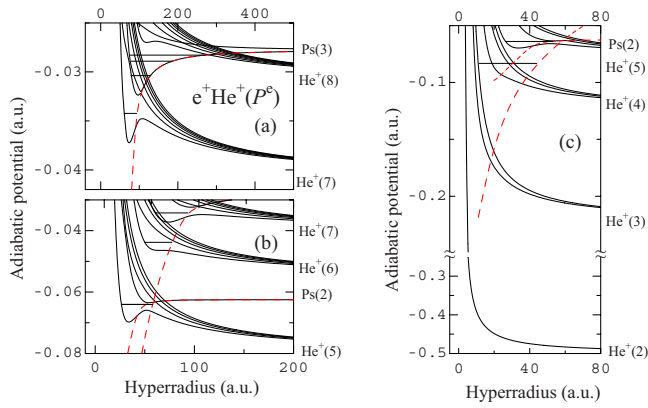


FIG. 5. (Color online) Adiabatic hyperspherical potentials of the system $e^+\text{He}^+(P^e)$ as functions of the hyper-radius. The vertical positions of the symbols $\text{He}^+(n)$ and $\text{Ps}(n)$ on the right roughly indicate these asymptotic threshold energies. For the broken curves and horizontal bars, see caption of Fig. 3.

Jacobi-coordinate close-coupling equations. Therefore, each infinite series of Feshbach resonances may be associated with an adiabatic hyperspherical potential. According to Table I, there exists one infinite series of dipole-supported $e^+\text{H}(P^e)$ resonances below each of the thresholds $\text{H}(n=3)$, $\text{H}(n=4)$, and $\text{Ps}(n=3)$ and two infinite series below $\text{H}(n=5)$. These numbers of series coincide with the numbers of the asymptotically attractive $e^+\text{H}(P^e)$ potentials seen in Fig. 3 below these thresholds. The potential approaching $\text{Ps}(n=2)$ is seen to be attractive, but it has no dipole tail and supports no infinite series, as has been noted in Sec. V. Inspection of Figs. 4–6 also reveals consistency with Table I as regard to the number of infinite series, though visual distinction of the weakly attractive dipole potentials from those decaying more rapidly than $\sim \rho^{-2}$ is sometimes difficult.

The energies E_r and widths Γ of the resonances lying below the threshold $\text{Ps}(n=3)$ and above the lower thresholds are plotted semilogarithmically in Fig. 7 for $e^+\text{H}(P^e)$ and $e^+\text{H}(D^o)$. Straight lines are also drawn with slopes $C = 1.115$ (for P^e) and 1.187 (for D^o), taken from Table I. The vertical positions of these lines are chosen to reproduce the higher members well, so that the parameters in Eq. (6) are

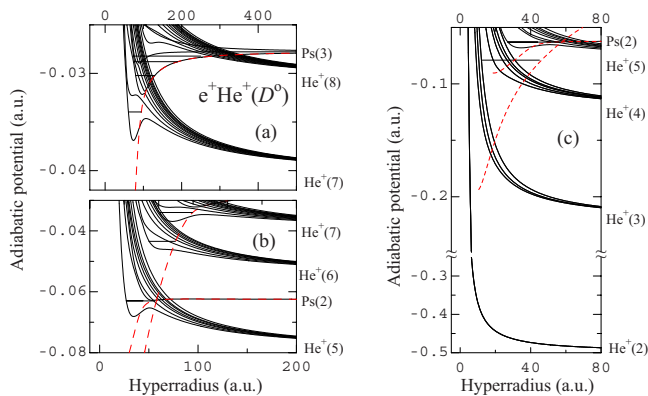


FIG. 6. (Color online) Adiabatic hyperspherical potentials of the system $e^+\text{He}^+(D^o)$ as functions of the hyper-radius. For the broken curves and horizontal bars, see caption of Fig. 3.

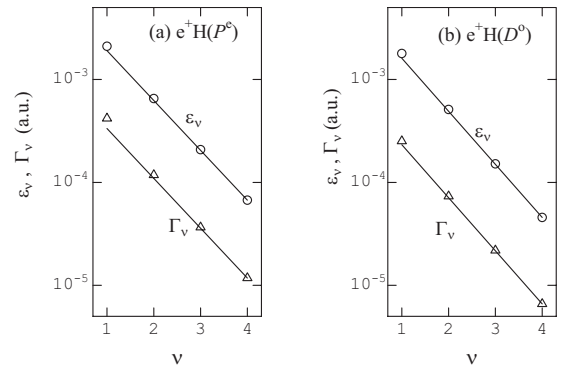


FIG. 7. Semilogarithmic plot of the positions $E_{r,\nu} = E_{\text{th}} - \varepsilon_\nu$ and widths Γ_ν of the (a) $e^+\text{H}(P^e)$ and (b) $e^+\text{H}(D^o)$ resonances below the $\text{Ps}(n=3)$ threshold $E_{\text{th}} = -0.027778$ and above the lower thresholds. The straight lines have slopes of 1.115 (for P^e) and 1.187 (for D^o) as taken from Table I. Their vertical positions are adjusted to reproduce the higher members of the resonance series.

estimated as $\varepsilon_0 \approx 6.0 \times 10^{-3}$ and $\Gamma_0 \approx 1.0 \times 10^{-3}$ for P^e and $\varepsilon_0 \approx 5.2 \times 10^{-3}$ and $\Gamma_0 \approx 7.6 \times 10^{-4}$ for D^o , though the second digit in these values could well be in some error.

The calculated resonance parameters are seen to satisfy Eq. (6) quite well with C common to both E_r and Γ . This corroborates clearly that, for both P^e and D^o , the four resonances belong to a common infinite series of dipole resonances. Indeed, Figs. 3(b) and 4(b) suggest that the lowest of the potentials with a breakup limit $p + \text{Ps}(n=3)$ supports these resonances. The energy points ε_1 in Figs. 7(a) and 7(b) for the lowest resonances slightly deviate above from the straight line, i.e., in the stronger binding direction, because these resonances are supported by the deep-well part of the potential, which is more attractive than the dipole potential. Nevertheless, even these resonances are seen to satisfy the dipole-resonance formula [Eq. (6)] fairly well. This is remarkable also because the avoided crossings of the supporting potential with other potential curves could have affected these resonances more strongly.

Similar observation is made for the three $e^+\text{He}^+(P^e)$ and three $e^+\text{He}^+(D^o)$ resonances below the threshold $\text{Ps}(n=3)$ and above the lower thresholds, plotted in Fig. 8 with open circles and triangles. The calculated results satisfy Eq. (6) quite well with slopes $C = 0.763$ (for P^e) and 0.786 (for D^o), taken from Table I. The energy values ε_1 are shifted slightly in the stronger binding direction, as is also the case with $e^+\text{H}$. The width Γ_1 for $e^+\text{He}^+(D^o)$ is fairly off the straight line, perhaps because of the avoided crossing of the lower part of the relevant adiabatic potential with a lower potential. The parameters in Eq. (6) are estimated as $\varepsilon_0 \approx 4.9 \times 10^{-3}$ and $\Gamma_0 \approx 2.9 \times 10^{-4}$ for P^e and $\varepsilon_0 \approx 4.5 \times 10^{-3}$ and $\Gamma_0 \approx 1.9 \times 10^{-4}$ for D^o , though the second digit could well be in some error.

Similar semilogarithmic analysis with the C values in Table I reveals that the two $e^+\text{H}(P^e)$ resonances below the threshold $\text{H}(n=3)$ belong to the infinite series with $C = 2.818$ and that the four $e^+\text{H}(P^e)$ resonances below $\text{H}(n=4)$ belong to the one with $C = 1.472$. The hyperspherical potentials supporting these series are obvious from Figs. 3(b) and 3(c) and Table I. Also, the three $e^+\text{H}(P^e)$ resonances

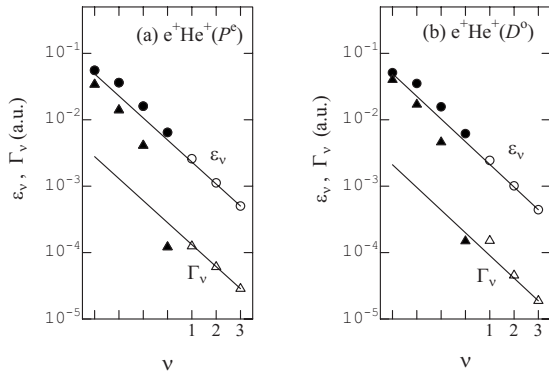


FIG. 8. Semilogarithmic plot of the positions $E_{r,\nu} = E_{\text{th}} - \varepsilon_\nu$ and widths Γ_ν of (a) the three $e^+\text{He}^+(P^e)$ and (b) the three $e^+\text{He}^+(D^o)$ resonances lying below the $\text{Ps}(n=3)$ threshold $E_{\text{th}} = -0.027\,778$ and above the lower thresholds (open circles and triangles). The straight lines have slopes of 0.7633 (for P^e) and 0.7862 (for D^o) as taken from Table I. Their vertical positions are adjusted to reproduce the higher members of the resonance series. Some lower-lying resonances are also included (solid circles and triangles) and discussed in Sec. VI C.

below $\text{H}(n=5)$ belong to the series with $C=1.027$ and are supported by the lowest potential in Fig. 3(a). Theoretically, there exists another series supported by the next lowest potential, as is clear from Table I. Nevertheless, it has failed to emerge in the calculation carried out so far.

A slightly more complicated case is the analysis of the five $e^+\text{H}(D^o)$ resonances below the threshold $\text{H}(n=5)$. In fact, they are classified into two groups. The three resonances that correspond to the three P^e resonances in Table II satisfy Eq. (6) with $C=1.065$. They are apparently supported by the lowest potential in Fig. 4(a). The other two resonances are found to be members of the series with $C=1.409$, supported by the next lowest potential. The third series associated with the weakly attractive potential in Fig. 4(a), which surely exists according to Table I, has escaped our detection so far.

Four $e^+\text{H}(D^o)$ resonances are found below $\text{H}(n=4)$ in Table II. All of them except for the third lowest ($-0.031\,54$) are analyzed to belong to the series with $C=1.597$, supported by the lowest potential in Fig. 4(b). The third lowest resonance may be regarded as supported by the second lowest potential. However, it may be affected by the avoided crossing of that potential with the next higher one. The $e^+\text{H}(D^o)$ resonance lying below $\text{H}(n=3)$ is most probably a member of the series with $C=4.388$ and is supported by the lowest of the three potentials approaching $\text{H}(n=3)$ in Fig. 4(c). However, no definite conclusion is drawn without locating other members of this series.

C. Diabatic picture for the resonance mechanism

The lowest-lying $e^+\text{He}^+(P^e)$ resonance at $-0.034\,23$ in Fig. 5(a) is an outstanding case challenging the generally accepted belief that resonances are supported by a minimum in an adiabatic hyperspherical potential with or without a barrier outside the minimum. This resonance occurs in the energy region of avoided crossing between two adiabatic

curves. It lies above the top of the barrier in the lower curve and below the dip of the upper curve.

In this avoided-crossing region of the energy and hyper-radius ρ the coupling between the two channels with avoided potentials should be crucial in unraveling the resonance mechanism. The essential dynamics must be determined by these two adiabatic channels. By a proper unitary transformation of them, a pair of diabatic channels may be created, which, if coupled, is equivalent to the pair of coupled adiabatic channels. One of the diabatic potentials should be connected from the outer-region ($\rho_x < \rho$) upper adiabatic potential to the inner-region ($\rho < \rho_x$) lower adiabatic potential smoothly across the diabatic crossing point ρ_x . This diabatic potential is attractive all the way inward through ρ_x until ρ reaches the minimum of the lower adiabatic potential. Beyond there, it follows the repulsive adiabatic potential. Then, this diabatic potential, say, $W_d(\rho)$, may support a bound state lying between the two avoided adiabatic potentials. This bound state must change into a resonance state due to the coupling with the other diabatic channel, producing a resonance unexpected from the adiabatic picture, such as the one at $-0.034\,23$.

This argument may be further supported from another aspect. Figure 5(a) suggests that the extension of the attractive part of the lowest $\text{Ps}(n=3)$ potential further down would approximate the attractive part of the diabatic potential $W_d(\rho)$ supporting the resonance at $-0.034\,23$. Then, this resonance may be regarded as another member of the infinite series of resonances lying below the threshold $\text{Ps}(n=3)$ and plotted in Fig. 8(a) with the open circles and triangles. Therefore, the data for this resonance are added to Fig. 8(a) by a solid circle and solid triangle to the left of and next to ε_1 and Γ_1 . Indeed, the resonance energy lies close to the straight line, demonstrating its membership of the same series. The width is off the straight line, which is quite reasonable since the width is very sensitive to the coupling with other channels, in general. The coupling associated with this resonance is quite different in nature from that associated with the upper members of the series.

A theoretical way of extrapolating the attractive part of the $\text{Ps}+\text{He}^{2+}$ potentials is to remove from the adiabatic potentials the contributions from the arrangement $e^++\text{He}^+$. This may be effected by constructing the basis functions for the adiabatic hyperspherical states $\varphi_i(\Omega;\rho)$ in terms only of the Jacobi coordinates for the arrangement $\text{Ps}+\text{He}^{2+}$ and by diagonalizing the adiabatic Hamiltonian matrix $H_{\text{ad}}(\Omega;\rho)$. The two lowest potential curves obtained in this way are included in Fig. 5 as broken curves. Thus, all the four resonances in Fig. 5(a) are visually understood to belong to the same series.

The D^o version of this unexpected resonance occurs at $-0.033\,96$ and is indicated as the lowest resonance in Fig. 6(a). This time three potential curves are seen to be involved in the avoided crossing. Nevertheless, the diabatic potential supporting this resonance is quite similar to the P^e case and is approximated by the broken curve obtained in the same way as the ones included in Fig. 5. The resonance energy and width are added to Fig. 8(b) by a solid circle and solid triangle to the left of and next to ε_1 and Γ_1 . Just as for the P^e symmetry, the resonance energy lies nearly on the straight

line, demonstrating its membership of the D^o series converging to the threshold $\text{Ps}(n=3)$.

The resonance at -0.0438 in Fig. 5(b) and the one at -0.04346 in Fig. 6(b) are also considered to be supported by the broken P^e (D^o) diabatic potential curve and hence regarded as a member of the P^e (D^o) infinite series. This is understood from the resonance parameters added to Figs. 8(a) and 8(b) (the third solid circle and triangle from left). Once again, the resonance energy lies close to the straight line in both of these figures. The width is quite large because of the strong coupling between the diabatic channels. Note the weak minimum structure in the lowest adiabatic potential curve tending to $\text{He}^+(n=6)$, revealing the strong avoided crossing with the $\text{Ps}(n=3)$ curve. The other $e^+ + \text{He}^+(n=6)$ potentials appear to be almost inactive in the presence of the $\text{He}^{2+} + \text{Ps}(n=3)$ channel.

Two diabatic broken curves are seen in Fig. 5(b) below the energy of $\text{Ps}(n=2)$, one approaching asymptotically to $\text{Ps}(n=2)$ and the other to $\text{Ps}(n=3)$. Each diabatic curve supports a resonance in this energy region. The one supported by the former occurs below and close to the threshold $\text{Ps}(n=2)$. This is a usual narrow independent Feshbach resonance. On the other hand, the resonance supported by the $\text{Ps}(n=3)$ diabatic potential is still another lower member of the series plotted in Fig. 8(a) (the second solid circle and triangle from left). It is naturally very broad and extends over a wide energy region across the threshold. This is the mechanism of the overlapping resonance analyzed in Sec. IV regarding Fig. 2. A similar overlapping resonance occurs also for the symmetry D^o [see Fig. 6(b) and the second solid circle and triangle from left in Fig. 8(b)].

The lowest resonance in Fig. 5(c), also shown in Fig. 1 as an example of a broad resonance, appears to be the lowest member of the series supported by the diabatic $\text{Ps}(n=3)$ potential of symmetry P^e . Naturally, its resonance energy [the leftmost solid circle in Fig. 8(a)] deviates significantly from the straight line since the part of the diabatic potential supporting this deep resonance level deviates significantly from the dipole form. Similarly, the lowest resonance in Fig. 6(c) appears to be the lowest member supported by the D^o diabatic $\text{Ps}(n=3)$ potential, though its resonance energy naturally deviates significantly from the straight line in Fig. 8(b).

VII. SUMMARY

Continuum states of unnatural parity $\pi=(-1)^{L+1}$ in the three-body systems $e^+\text{H}$ and $e^+\text{He}^+$ have been studied. Unlike natural-parity states, they contain no two-body s -state component. As a consequence of this, the continuum begins from the energy of the $\text{H}(2p)$ or $\text{He}^+(2p)$ state, no infinite series of Feshbach resonances exist below the threshold of the $\text{Ps}(2p)$ state, and the lowest-order 2γ and 3γ pair annihilation is forbidden.

The infinite resonance series converging to the thresholds $\text{H}(n\geq 3)$ and $\text{Ps}(n\geq 3)$ are supported by the diagonalized asymptotic dipole potentials in the Jacobi coordinates. These dipole potentials correspond approximately one to one to the asymptotic part of adiabatic hyperspherical potentials. Thus, an infinite series is associated with a hyperspherical potential. Based on the theoretical common ratios of the geometric progressions representing the resonance positions and widths of the infinite series, many of the calculated resonances have been identified to be members of a particular series and hence supported by a particular adiabatic potential. Several resonances are unassociated with a minimum of any single adiabatic potential. They have been interpreted as supported by a diabatic hyperspherical potential. The outer attractive part of this diabatic potential may be approximated by extending the attractive part of an adiabatic potential downward. Thus, some of these resonances may be regarded as low-lying members of the infinite series, of which the higher members are supported by a dipole potential. Broad and narrow resonances sometimes happen to overlap each other, the former being such a low-lying member of an infinite series and the latter being supported by another diabatic potential.

ACKNOWLEDGMENTS

One of the authors (I.S.) wishes to acknowledge with gratitude the support and the kind hospitality extended by the Advanced Science Research Center, Japan Atomic Energy Agency and its director, Professor Y. Hatano.

-
- [1] See, e.g., J. Midtdal, Phys. Rev. **138**, A1010 (1965); G. W. F. Drake, M. M. Cassar, and R. A. Nistor, Phys. Rev. A **65**, 054501 (2002); M. Bylicki and E. Bednarz, *ibid.* **67**, 022503 (2003), and references therein.
- [2] J. Mitroy and M. W. J. Bromley, Phys. Rev. Lett. **98**, 063401 (2007).
- [3] M. W. J. Bromley, J. Mitroy, and K. Varga, Phys. Rev. A **75**, 062505 (2007).
- [4] J. M. Richard, Phys. Rev. A **67**, 034702 (2003).
- [5] M. V. Zhukov, B. V. Danilin, D. V. Fedorov, J. M. Bang, I. S. Thompson, and J. S. Vaagen, Phys. Rep. **231**, 151 (1993).
- [6] Z.-C. Yan and Y. K. Ho, Phys. Rev. A **77**, 030701(R) (2008).
- [7] Y. K. Ho and Z.-C. Yan, J. Phys. B **42**, 044006 (2009).
- [8] J. H. Macek, J. Phys. B **1**, 831 (1968).
- [9] C. D. Lin, Phys. Rep. **257**, 1 (1995).
- [10] J.-Z. Tang, S. Watanabe, and M. Matsuzawa, Phys. Rev. A **46**, 2437 (1992); J.-Z. Tang, S. Watanabe, M. Matsuzawa, and C. D. Lin, Phys. Rev. Lett. **69**, 1633 (1992); Y. Zhou and C. D. Lin, J. Phys. B **27**, 5065 (1994).
- [11] A. Igarashi and N. Toshima, Phys. Rev. A **50**, 232 (1994); A. Igarashi, N. Toshima, and T. Shirai, *ibid.* **50**, 4951 (1994).
- [12] J.-Z. Tang and I. Shimamura, Phys. Rev. A **50**, 1321 (1994); **51**, R1738 (1995); **52**, R3413 (1995); J.-Z. Tang, C. D. Lin, B. Zhou, and I. Shimamura, *ibid.* **51**, 4694 (1995).
- [13] Y. Zhou and C. D. Lin, Phys. Rev. Lett. **75**, 2296 (1995); Anh-Thu Le, M. W. J. Bromley, and C. D. Lin, Phys. Rev. A

- 71**, 032713 (2005); Anh-Thu Le, T. Morishita, X.-M. Tong, and C. D. Lin, *ibid.* **72**, 032511 (2005).
- [14] D. Kato and S. Watanabe, Phys. Rev. A **56**, 3687 (1997).
- [15] A. Igarashi and I. Shimamura, Phys. Rev. A **56**, 4733 (1997); A. Igarashi, I. Shimamura, and N. Toshima, *ibid.* **58**, 1166 (1998); A. Igarashi and I. Shimamura, *ibid.* **70**, 012706 (2004).
- [16] For applications to heavy-particle collisions, see A. Igarashi and N. Toshima, Eur. Phys. J. D **46**, 425 (2008), and references therein.
- [17] J. M. Blatt and V. F. Weisskopf, *Theoretical Nuclear Physics* (Springer, New York, 1979), Chap. X.
- [18] A. U. Hazi, Phys. Rev. A **19**, 920 (1979).
- [19] F. T. Smith, Phys. Rev. **118**, 349 (1960).
- [20] A. Igarashi and I. Shimamura, J. Phys. B **37**, 4221 (2004).
- [21] I. Shimamura, J. F. McCann, and A. Igarashi, J. Phys. B **39**, 1847 (2006).
- [22] K. Aiba, A. Igarashi, and I. Shimamura, J. Phys. B **40**, F9 (2007).
- [23] M. Gailitis and R. Damburg, Proc. Phys. Soc. London **82**, 192 (1963).